

Kicked Bose-Hubbard systems and kicked tops – destruction and stimulation of tunneling

M P Strzys, E M Graefe and H J Korsch

FB Physik, Technische Universität Kaiserslautern, D-67653 Kaiserslautern, Germany

E-mail: korsch@physik.uni-kl.de

Abstract. In the two-mode approximation Bose-Einstein condensates (BEC) in a double-well potential can be described by a many particle Hamiltonian of Bose-Hubbard type. We focus on such a BEC whose interatomic interaction strength is modulated periodically with δ -kicks. This System in fact represents a model of a kicked top. The mean-field dynamics provide a rich mixed phase space with regular and chaotic regions. By increasing the kick-strength a bifurcation leads to the appearance of self-trapping states localized in regular islands. This self-trapping is also found for the many particle system, however in general suppressed by tunneling oscillations. We show that the tunneling time can be calculated from the quasi-energy splitting of the corresponding Floquet states. By varying the kick-strength these quasi-energy levels undergo both avoided and even real crossings. Therefore stimulation or actually complete destruction of tunneling is observed for this many particle system.

PACS numbers: 03.65.-w, 03.75.Lm, 05.45.Mt

1. Introduction

After their first experimental realization [1, 2] Bose-Einstein condensates (BEC) have stimulated an enormous amount of theoretical investigations. Especially the recent progress in confining and manipulating BECs [3, 4] has opened the opportunity of realising many kinds of quantum mechanical models.

Since a full many-particle treatment of BECs is usually only possible for a very small number of atoms, such systems are mostly described according to the celebrated mean-field approximation, which describes the system quite well for large particle numbers at low temperatures. A huge number of previous studies focussed on relatively simple models like the two mode system in order to investigate the correspondence between many-particle and mean-field description. Most interestingly the mean-field description as large particle number limit of many-particle systems is formally related to the usual classical limit of quantum mechanics. In a number of recent papers consequences of the classical nature of the mean-field approximation are discussed and semiclassical aspects are introduced [5–9]. For a double-well system even the eigenenergies and eigenstates of the many-particle system could be reconstructed approximately from the mean-field system in a WKB type manner with astonishing accuracy [9]. Recently especially experiments with a relatively small number of particles [3] offer a nice opportunity to study the interplay of classical and essential quantum behaviour.

Within the theory of quantum chaos systems with a periodic time dependence play an important role. Despite their apparently academic character especially systems with a delta-type time dependence are of particular relevance. Their prominence is not only due to their relatively simple handling but first of all to their archetypical behavior. Therefore systems like the kicked rotor or the kicked top became standard models in this area.

In the present paper we focus on a N -particle Bose-Einstein condensate in a double-well trap with a periodic kicked interaction strength. In a two-mode approximation such a system can be described by a two-site Bose-Hubbard type Hamiltonian. In the case of a symmetric trap this model is in fact the Hamiltonian of a kicked top studied by Haake *et al.* in the context of quantum chaos [10, 11] which has actually become a standard model in this area. Considering this BEC context the question if the kicked top could be realised experimentally [12] can be answered in a novel way. This new context offers as well the opportunity to study aspects of the system which were not investigated in the past.

One of the most prominent features of the corresponding time independent system is the so called self-trapping effect [13]. Above a critical value of the interaction strength the system properties change qualitatively and unbalanced solutions appear, favoring one of the wells. A careful discussion of this effect, the relation between mean field and N -particle behavior as well as its control by external driving fields can be found in [14]. In the many-particle system this effect is suppressed by tunneling oscillations. The same effect is as well present in the kicked system. In that case the dynamics of

the many-particle system is much richer. In fact a whole bunch of archetypical features of quantum dynamical systems like coherent destruction of tunneling and chaos assisted tunneling can be found in this model.

In the following we present the basic model in section 2 and give a short review of the Floquet formalism in section 3. Afterwards we first investigate the mean-field dynamics in section 4 and then compare it to the much richer many-particle dynamics in section 5. We conclude the paper with a detailed discussion of the tunneling behavior of the model.

2. The basic model

The Hamiltonian of the Bose-Hubbard-system we focus on

$$H(t) = \frac{\varepsilon}{2} (a_1^\dagger a_1 - a_2^\dagger a_2) + \frac{v}{2} (a_1^\dagger a_2 + a_2^\dagger a_1) - \frac{c(t)}{4} (a_1^\dagger a_1 - a_2^\dagger a_2)^2 \quad (1)$$

includes a time periodic kicked interaction strength $c(t) = c \sum_n \delta(t - n)$.

Introducing three angular momentum operators according to the Schwinger representation

$$L_x = \frac{1}{2} (a_1^\dagger a_2 + a_2^\dagger a_1), L_y = \frac{1}{2i} (a_1^\dagger a_2 - a_2^\dagger a_1), L_z = \frac{1}{2} (a_1^\dagger a_1 - a_2^\dagger a_2) \quad (2)$$

which obey the usual $su(2)$ commutation relations $[L_i, L_j] = iL_k$, where $i, j, k = x, y, z$ and cyclic permutations, the Hamiltonian (1) assumes the form

$$H(t) = \varepsilon L_z + v L_x - c(t) L_z^2 = H_0 + c(t) V. \quad (3)$$

In the case $\varepsilon = 0$ this is in fact the Hamiltonian of a kicked top. A similar system with kicked single particle tunnelling v has been studied in [15].

3. Quantum-Floquet Formalism

Since the Hamiltonian (1) is periodic in time, $H(t + \tau) = H(t)$, it is useful to introduce the propagator over one period, the so called Floquet-operator

$$F(t) = U(t + \tau, t) = \mathcal{T} \left[\exp \left(-i \int_t^{t+\tau} H(t') dt' \right) \right] \quad (4)$$

where the operator \mathcal{T} takes care of the right time order. According to the δ -type time dependence the Floquet-operator factorizes and a similar expression would be obtained by modulating the single particle tunneling coupling v with periodic δ -kicks instead of the particle interaction c . For convenience we introduce the operator

$$F = F(0) = e^{icL_z^2\tau} e^{-i(\varepsilon L_z + v L_x)\tau}. \quad (5)$$

The Floquet operator (4) is by definition unitary and thus has unimodular eigenvalues

$$F(t) |\kappa(t)\rangle = e^{-i\epsilon_\kappa \tau} |\kappa(t)\rangle. \quad (6)$$

The $N + 1$ quasi-energies ϵ_κ are the natural counterpart of the energies of time-independent systems. We always choose ϵ_κ in the first Brillouin-zone $[-\pi/\tau, \pi/\tau]$.

The eigenstates of the Floquet-operator, the so called Floquet-states $|\kappa(t)\rangle$ form an orthonormal basis of the Hilbert space and obey

$$|\kappa(t)\rangle = e^{-i\epsilon_\kappa t} |\phi_\kappa(t)\rangle, \quad (7)$$

similar to Bloch-waves in the case of spatially periodic potentials. They factorize into a phase factor and a part periodic in time, $\phi_\kappa(t + \tau) = \phi_\kappa(t)$.

The additional symmetry in the case of a symmetric double-well with $\varepsilon = 0$ can be expressed via an invariance under rotations $R_x = R_x(\pi) = e^{-i\pi L_x}$ around the x -axis about π . The Floquet operator commutes with R_x ,

$$[F, R_x] = 0, \quad (8)$$

and the Floquet states can be separated into two symmetry classes, one even and one odd under the rotation R_x . If N is even, the angular momentum quantum number l is an integer. Thus we have $R_x^2 = \mathbb{1}$ and the eigenvalues of R_x are ± 1 . Equation (6) can be reformulated according to

$$F |\kappa_\pm\rangle = e^{-i\epsilon_\kappa \tau} |\kappa_\pm\rangle \quad (9)$$

where

$$R_x |\kappa_\pm\rangle = \pm |\kappa_\pm\rangle. \quad (10)$$

On the other hand, if N is odd $R_x^2 = -\mathbb{1}$ holds, since l is half an integer. The eigenvalues of R_x then are $\pm i$. This yields as well two classes of Floquet states $|\kappa\rangle$, which obey

$$R_x |\kappa_\pm\rangle = \pm i |\kappa_\pm\rangle. \quad (11)$$

These two symmetry classes will be of great interest concerning the tunneling process that is investigated in the following.

4. Mean-field Dynamics

The celebrated mean-field approximation can be achieved by replacing the field operators by complex numbers by the means of

$$a_j \longrightarrow \psi_j, \quad a_j^\dagger \longrightarrow \psi_j^*, \quad j = 1, 2. \quad (12)$$

These two regimes are connected via a semiclassical relationship, where the parameter $1/N$ takes over the role of an effective Planck constant. Thus, the limit $1/N \rightarrow 0$ leads to the mean-field approximation. However the mapping (12) is not unique, since complex numbers commute. Therefore, we complete the mapping (12) with the additional rule [7, 9]

$$\frac{a_j^\dagger a_j + a_j a_j^\dagger}{2} \longrightarrow |\psi_j|^2, \quad j = 1, 2. \quad (13)$$

In the case of the Hamiltonian (1) this mapping leads to a classical Hamiltonian function

$$\mathcal{H}(\psi_{1,2}, \psi_{1,2}^*) = \frac{\varepsilon}{2}(\psi_1^*\psi_1 - \psi_2^*\psi_2) + \frac{v}{2}(\psi_1^*\psi_2 + \psi_2^*\psi_1) - \frac{c(t)}{4}(\psi_1^*\psi_1 - \psi_2^*\psi_2)^2 \quad (14)$$

of the conjugate variables ψ_j and ψ_j^* . Notice that, due to the rule (13), the mean-field wave-function is normalized according to $|\psi_1|^2 + |\psi_2|^2 = N + 1$ which is crucial because of the nonlinear selfinteraction term in (14).

The dynamics of such a system is governed by the discrete Gross-Pitaevskii equation (GPE), also called nonlinear Schrödinger equation, that can be written in terms of a nonlinear matrix equation

$$i \frac{d}{dt} \begin{pmatrix} \psi_1(t) \\ \psi_2(t) \end{pmatrix} = \frac{1}{2} \begin{pmatrix} \varepsilon + c(t)\kappa & v \\ v & -(\varepsilon + c(t)\kappa) \end{pmatrix} \begin{pmatrix} \psi_1(t) \\ \psi_2(t) \end{pmatrix}, \quad (15)$$

where $\kappa = |\psi_2|^2 - |\psi_1|^2$ is the population imbalance of the two wells. The dynamics described by this equation of motion is Hamiltonian and conserves the norm of the wave-function. A nice possibility to visualize the dynamics is a mapping onto the Bloch sphere. Similar to (2), one defines the three quantities

$$s_x = \frac{1}{2}(\psi_1^*\psi_2 + \psi_1\psi_2^*), \quad s_y = \frac{1}{2i}(\psi_1^*\psi_2 - \psi_1\psi_2^*), \quad s_z = \frac{1}{2}(|\psi_1|^2 - |\psi_2|^2), \quad (16)$$

the components of the Bloch vector $\mathbf{s} \in \mathbb{R}^3$. The norm of the Bloch vector $|\mathbf{s}| = s = (N + 1)/2$ is determined by the normalization of the mean-field wave-function. Writing the GPE (15) in terms of the Bloch vector yields the nonlinear Bloch equations

$$\begin{aligned} \dot{s}_x &= -\varepsilon s_y + 2c(t)s_y s_z \\ \dot{s}_y &= \varepsilon s_x - v s_z - 2c(t)s_x s_z \\ \dot{s}_z &= v s_y. \end{aligned} \quad (17)$$

In analogy to the many particle case one can define a Floquet operator for the mean-field Bloch vector which follows the stroboscopic mapping

$$\mathbf{s}_{n+1} = F\mathbf{s}_n = KR\mathbf{s}_n \quad (18)$$

of the dynamics, where $\mathbf{s}_n = \mathbf{s}(n\tau)$, $n \in \mathbb{Z}$. In this mean-field approximation the Floquet operator again factorizes into a rotation R about the axis $(v/\omega, 0, \varepsilon/\omega)$ and a torsion K along the z -direction. Stroboscopic iterations of \mathbf{s} according to the discrete mapping (18) for a symmetric double-well potential ($\varepsilon = 0$) with $v = 1$ and four different values of the interaction-strength c are presented in figure 1. In dependence of the control parameter c , the system exhibits the typical behaviour of classical nonlinear and thus chaotic systems. In the case of no interaction ($c = 0$) shown in a) one observes the usual Rabi oscillations which give rise to simple rotations of the Bloch vector. At the two stable fixed points $(\pm s, 0, 0)$ the population imbalance of the two wells is constant in time. With increasing interaction the linear rotation around the x -axis is more and more perturbed by a torsion along the z -axis and bifurcations of the fixed points occur. For $c = 1.1/(N + 1)$, shown in b), the first bifurcation of the fixed point $(-s, 0, 0)$ has just caused two new fixed points to appear. Increasing c further, the regular islands

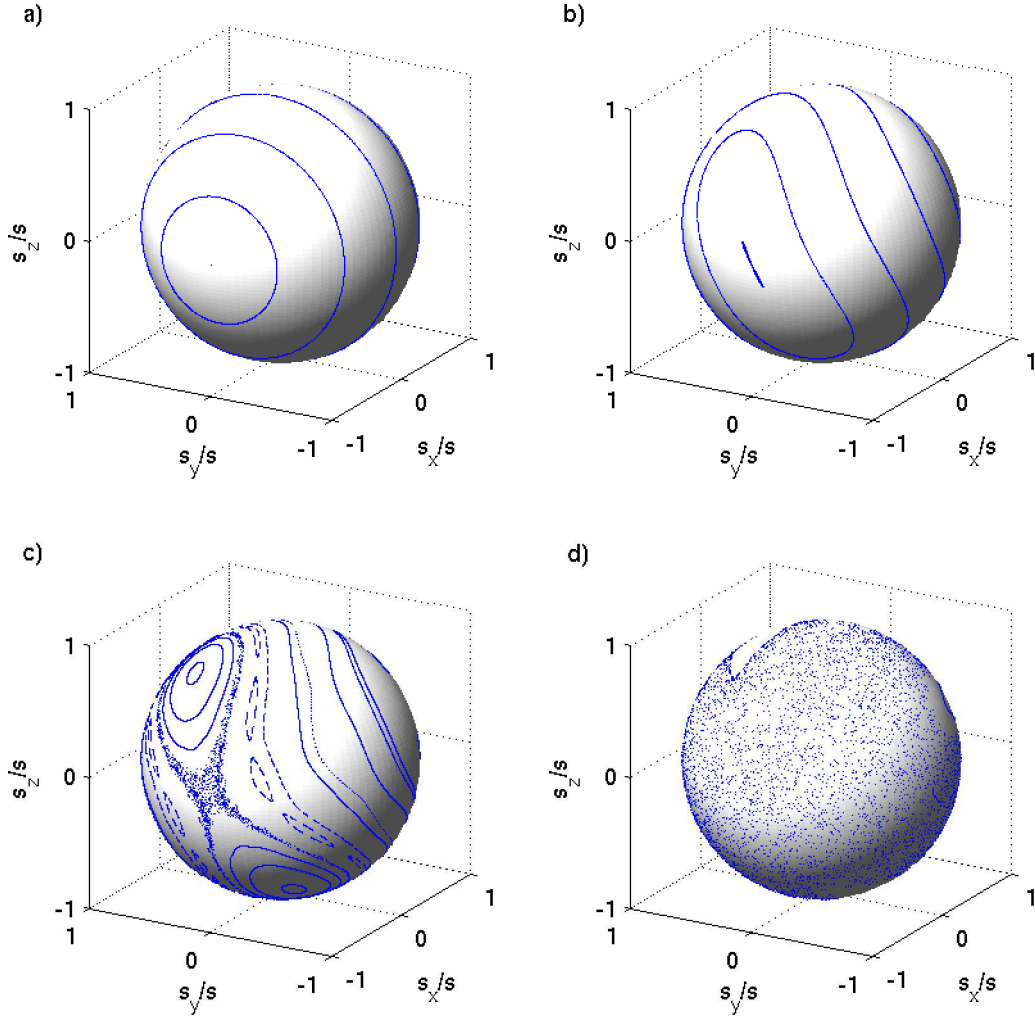


Figure 1. Stroboscopic dynamics of the Bloch vector \mathbf{s} for the parameters $\varepsilon = 0$, $v = 1$, $\tau = 1$ and a) $c = 0$, b) $c = 1.1/(N+1)$, c) $c = 1.8/(N+1)$ and d) $c = 3.5/(N+1)$, respectively

around the new fixed points grow while the fixed points wander towards the poles of the Bloch sphere; the example $c = 1.8/(N+1)$ can be seen in c). These two regular islands will be of special interest in the following, since they correspond to the famous self-trapping states of the non-kicked system as they are localized on the northern and southern hemisphere, respectively. Unlike the non-kicked system, self-trapping occurs only in a certain regime, since increasing c even further leads inevitably to global chaos. The case $c = 3.5/(N+1)$ is shown in d); the chaotic sea spreads noticeably over almost the whole sphere, sparing only small shrinking regular islands.

The critical value of the parameter c for the occurrence of self-trapping, i. e. the point of bifurcation of the prominent fixed point $(-s, 0, 0)$, can be calculated in dependence of the other system parameters by linearization. To guarantee stability of

the fixed point $(-s, 0, 0)$ the interaction strength must obey the inequalities

$$\frac{\cos v\tau \pm 1}{s \sin v\tau} < c < \frac{\cos v\tau \mp 1}{s \sin v\tau} \quad \text{for} \quad \sin v\tau \gtrless 0. \quad (19)$$

Thus, for parameters $\tau = v = 1$, this fixed point is stable for $c \in (-3.661, 1.092)/(N+1)$.

5. Many particle quantum dynamics

In order to compare the mean-field dynamics with the full quantum dynamics, we introduce the $SU(2)$ coherent states, also called atomic coherent states $|\vartheta, \varphi\rangle$. They are constructed by acting an arbitrary $SU(2)$ -rotation $R(\vartheta, \varphi) = \exp i\vartheta(L_x \sin \varphi - L_y \cos \varphi)$ on the extremal Fock state $|N\rangle$ with all particles in the first well, which is a coherent state located at the north pole of the Bloch sphere [16, 17],

$$|\vartheta, \varphi\rangle = R(\vartheta, \varphi) |N\rangle. \quad (20)$$

In the Fock basis they take the form

$$|\vartheta, \varphi\rangle = \sum_{n=0}^N \sqrt{\binom{N}{n}} \cos^n \left(\frac{\vartheta}{2}\right) \sin^{N-n} \left(\frac{\vartheta}{2}\right) e^{i(N-n)\varphi} |n\rangle, \quad (21)$$

where

$$|n\rangle = |n, N-n\rangle = \frac{1}{\sqrt{n!(N-n)!}} (a_1^\dagger)^n (a_2^\dagger)^{N-n} |0, 0\rangle, \quad (22)$$

with $n = 0, 1, \dots, N$ are the usual Fock states. The expectation values of the angular momentum operators in a coherent state $\langle L_j \rangle = \langle \vartheta, \varphi | L_j | \vartheta, \varphi \rangle$, $j = x, y, z$ are given by

$$\langle L_x \rangle = \frac{N}{2} \sin \vartheta \cos \varphi, \quad \langle L_y \rangle = \frac{N}{2} \sin \vartheta \sin \varphi, \quad \langle L_z \rangle = \frac{N}{2} \cos \vartheta. \quad (23)$$

Thus, the vector $\langle \mathbf{L} \rangle = (\langle L_x \rangle, \langle L_y \rangle, \langle L_z \rangle)$ points on a sphere with radius $l = N/2$.

Here again, the Floquet operator induces a discrete mapping from kick to kick. In the Heisenberg picture this yields the mapping

$$L_j^{(m+1)} = F^\dagger L_j^{(m)} F = e^{iH_0\tau} \left(e^{icV\tau} L_j^{(m)} e^{-icV\tau} \right) e^{-iH_0\tau} \quad (24)$$

for the angular momentum operators. In the case of symmetric double-wells with $\varepsilon = 0$ these equations assume the simple form

$$\begin{aligned} F^\dagger L_x F &= \frac{1}{2} \left[(L_x + i(L_y \cos v\tau - L_z \sin v\tau)) e^{-ic(1+2L_y \sin v\tau+2L_z \cos v\tau)} \right] \\ &\quad + \text{h.c.} \\ F^\dagger L_y F &= \frac{1}{2i} \left[(L_x + i(L_y \cos v\tau - L_z \sin v\tau)) e^{-ic(1+2L_y \sin v\tau+2L_z \cos v\tau)} \right] \\ &\quad + \text{h.c.} \\ F^\dagger L_z F &= L_y \sin v\tau + L_z \cos v\tau. \end{aligned} \quad (25)$$

Now we can compare the mean-field with the many particle dynamics. For this purpose we compare the normalized Bloch vector \mathbf{s}/s with the normalized vector of expectation values of the angular momentum operators $\langle \mathbf{L} \rangle /l$. In the classically regular

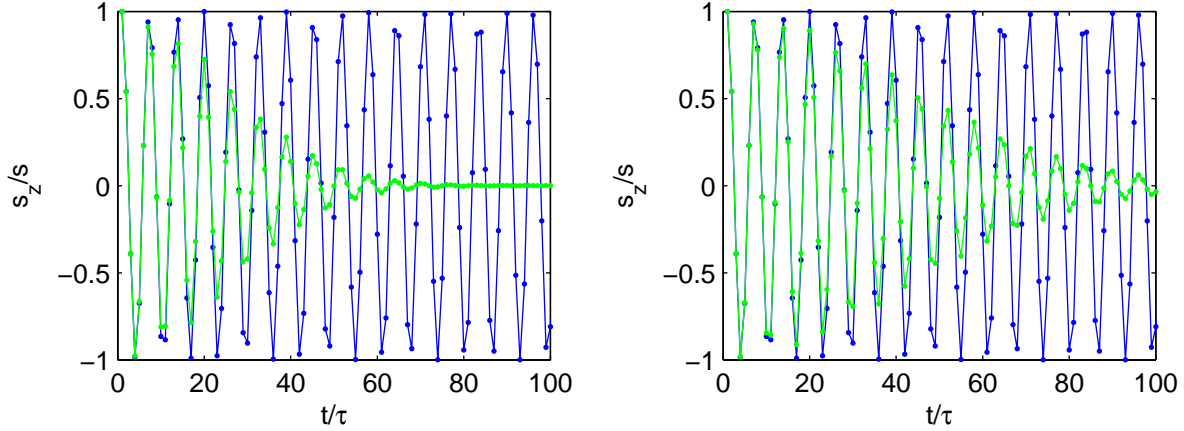


Figure 2. Comparison of the evolution of the z -component of a state initially equal to the coherent state $|N\rangle$ located at the north pole for the set of parameters $\varepsilon = 0$, $v = 1$, $\tau = 1$ and $c = 0.5/(N + 1)$; starting vector: $\mathbf{s}/s = \mathbf{x} = (0, 0, 1)$; ● mean-field, ● full quantum dynamics (the lines are plotted to guide the eye); left: $N = 33$ particles, right: $N = 100$ particles.

regime, the full quantum dynamics are closely resembling the mean-field system and shows the usual Rabi oscillations modulated by a breakdown and revival scenario due to the discrete spectrum of the system. A similar behaviour is very common and known for many systems [18]. Figure 2 shows this comparison for a symmetric double-well potential ($\varepsilon = 0$) and $v = \tau = 1$ for a small interaction strength $c = 0.5/(N + 1)$, where initially the state is a coherent state $|N\rangle$ located at the north pole, or $\mathbf{s}/s = (0, 0, 1)$ in the mean-field approximation.

Our interest, however, is not focused on the regular regime, but on the mixed regular-chaotic regime with the two prominent regular islands centered at the self-trapping states $\mathbf{s}_\pm = \mathbf{s}(\vartheta_\pm, \varphi_\pm)$. A mean-field trajectory started in one of these states will stay there forever. The full quantum system shows a much richer behaviour here. Starting the propagation in one of the corresponding coherent states $|\pm\rangle = |\vartheta_\pm, \varphi_\pm\rangle$ the system exhibits dynamical tunneling to the other island, i. e. the state $|\mp\rangle$. This periodically repeating process is known for many systems, e.g. one particle in periodically driven double-well potential [19–21], a periodically driven pendulum [22, 23]. Such a system can be realized with a BEC [24–28] allowing direct experimental observation of the tunneling. In figure 3 the tunneling process starting from the fixed point on the southern hemisphere in the state $|\psi(0)\rangle = |-\rangle$ is shown for several parameter sets. An interaction strength of $c = 2/(N + 1)$ is chosen to ensure the two regular islands to be not too small and the distance of the fixed points to be large. One observes dynamical tunneling through the Bloch sphere. The normalized expectation value $\langle \mathbf{L} \rangle / l$ spirals its way on a tube around a straightline connecting the two island states to the other side of the sphere. With increasing number of particles the tunneling takes a longer time. The radius of the tunneling tube is determined by the uncertainty of the direction of the angular momentum vector in a coherent state, which is proportional

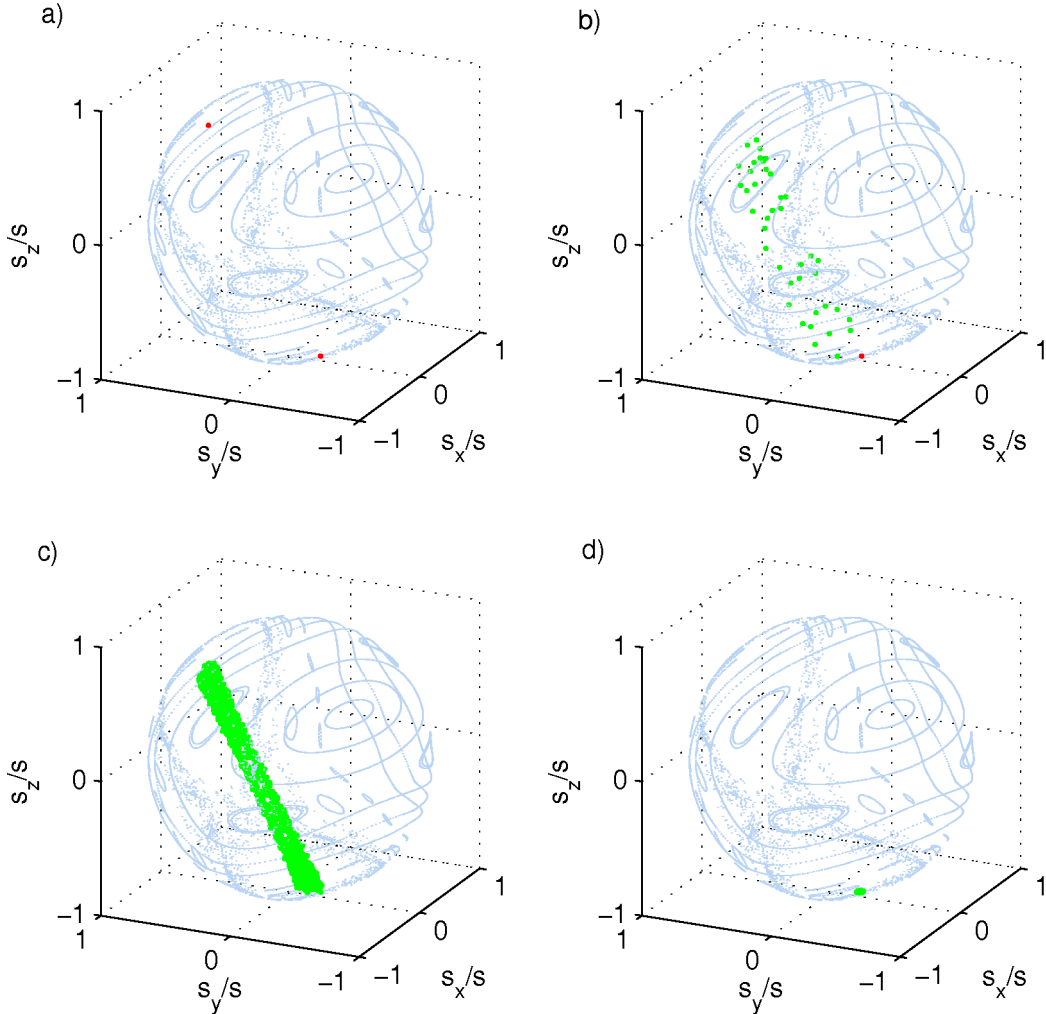


Figure 3. a) mean-field phase space for the parameters $\varepsilon = 0$, $v = 1$, $\tau = 1$ und $c = 2/(N+1)$, the fixed points s_{\pm} are marked with red dots; b) propagation of $|\rightarrow\rangle$ for $N = 10$ particles; the tunneling to the northern fixed point lasts 40 periods here; c) as before, but $N = 20$ particles; tunneling during 1000 periods d) as in c), but $N = 100$ particles, tunneling cannot be observed here.

to $1/N$. The more particles one puts into the system, the tighter is the spiral around the connection line of the fixed points. One could get the impression of the tunneling time to increase monotonically with increasing number of particles. This however is actually wrong as the system exhibits interesting features which are the main interest of our studies. But let us first have a closer look on the tunneling process. We analyze the squared absolute values $|\langle\psi(t)|\pm\rangle|^2$ of the projections of $|\psi(t)\rangle$ on the coherent island states and the orthogonal subspace for the case c) of figure 3 with $N = 20$ during propagation, see figure 4. After 1000 periods, the population has been transferred almost completely to the state $|+\rangle$ on the northern hemisphere.

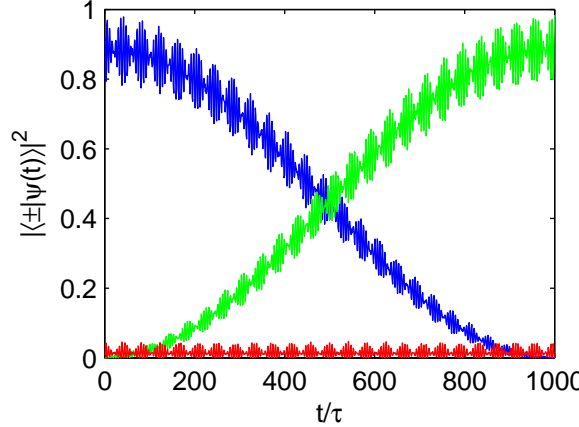


Figure 4. Squared absolute values of the projections of $|\psi(t)\rangle$ on the coherent states $|\pm\rangle$ during propagation over 1000 periods for $N = 20$ particles, $\varepsilon = 0$, $v = 1$, $\tau = 1$ and $c = 2/(N + 1)$; — $|\langle -|\psi(t)\rangle|^2$, — $|\langle +|\psi(t)\rangle|^2$ and — orthogonal subspace

The squared absolute value of the projection $|\langle \kappa_- | \rangle|^2$ of the southern island state on the Floquet states $|\kappa\rangle$ is significantly large only for two of the $(N + 1)$ Floquet states which are denoted by $|\kappa_{\pm}\rangle$. As indicated by the sign, they belong to different symmetry classes. With the help of those states, the island states can be reconstructed up to 94 % by the linear combinations

$$|\psi_{\pm}\rangle = -\frac{1}{\sqrt{2}} (|\kappa_+\rangle \pm |\kappa_-\rangle) \quad (26)$$

which hence are a good approximation for the coherent states $|\pm\rangle \approx |\psi_{\pm}\rangle$. If one chooses $|\psi_-\rangle$ as a starting vector, $|\psi(t)\rangle$ always stays a linear combination of $|\kappa_{\pm}\rangle$ during propagation. Therefore, the tunneling leads along the connection line of the two fixed points. Thus the spiraling is due to the other contributing Floquet states.

One might conclude, that the subsystem consisting of the two island states $|\pm\rangle$ can be described as a two state system of the Floquet states $|\kappa_{\pm}\rangle$ in a good approximation. Then the tunneling can also be treated analogously to a two level system. Thus the system exhibits periodic tunneling and the tunneling period T_{tunnel} can immediately be determined to be

$$T_{\text{tunnel}} = \frac{2\pi}{\epsilon_- - \epsilon_+} = \frac{2\pi}{\Delta\epsilon}. \quad (27)$$

All these considerations are entirely equivalent to the tunneling process through a symmetric potential barrier, where the quasi energies adopt the function of the energies of time independent systems. Thus the tunneling period is solely ruled by the quasi energy splitting $\Delta\epsilon$. The tunneling between the two island states corresponds to an actual tunneling of the BEC from one potential well to the other. Is the system localized in the southern island $|-\rangle$ the expectation value of L_z is negative and the condensate is located mainly in the second well; in the case $c = 2/(N + 1)$ over 80 % of the condensate are trapped there. The opposite is true for the northern island $|+\rangle$.

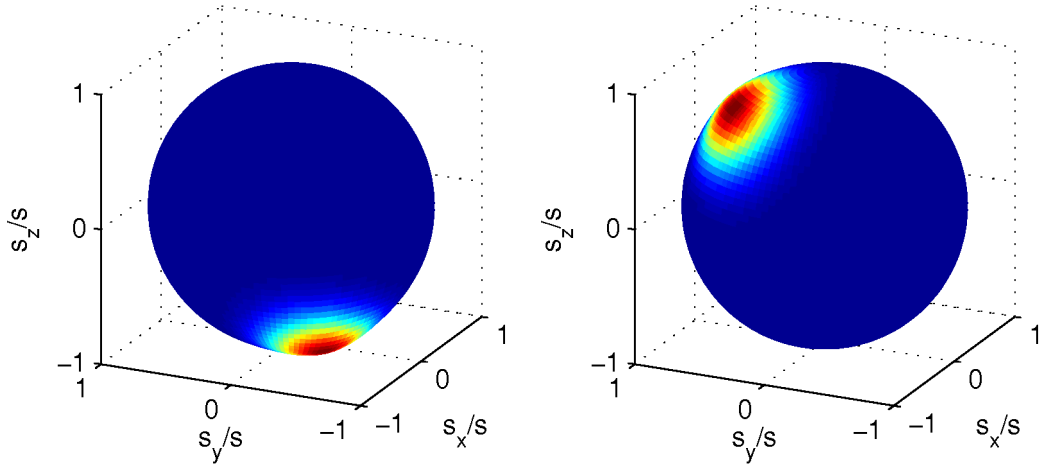


Figure 5. Husimi distributions of the island states $|\psi_{\pm}\rangle$; left: $Q_-(\vartheta, \varphi) = |\langle \vartheta, \varphi | \psi_- \rangle|^2$, right: $Q_+(\vartheta, \varphi) = |\langle \vartheta, \varphi | \psi_+ \rangle|^2$ for $N = 20$ particles, $\varepsilon = 0$, $v = 1$, $\tau = 1$ and $c = 2/(N + 1)$

To give an impression of the localization of the Floquet states, one can compute quantum phase space distributions, e.g. the Husimi distributions [29]

$$Q(\vartheta, \varphi) = |\langle \vartheta, \varphi | \psi \rangle|^2. \quad (28)$$

via the $SU(2)$ coherent states $|\vartheta, \varphi\rangle$. In figure 5 the Q -function for the linear combinations $|\psi_{\pm}\rangle$ of the two Floquet tunneling states are shown. The sharp localization in on of the two regular islands is evident here.

5.1. Parameter dependencies of T_{tunnel}

In general the dynamics of the island states however is more complicated and shows special features. Tunneling can in fact be extremely stimulated or fully suppressed as we will see now. At first we examine the tunneling for different numbers of particles. In fig. 6 the tunneling period T_{tunnel} for fixed $c = 2/(N + 1)$ calculated with the help of (27) is plotted over N ; please note the logarithmic scaling of the T -axis. This is in excellent agreement with the tunneling time directly determined from the propagation, plotted in red here. For small N the tunneling period increases exponentially. For larger N new structures appear, where the tunneling time decreases rapidly about several orders of magnitude. These “resonances” have been observed for other systems e.g. the anharmonic driven oscillator [19, 22, 30]. In general this phenomenon can be explained with an avoided crossing of the tunneling doublet ϵ_{\pm} with some third level ϵ_c which increases the splitting $\Delta\epsilon$. In such regions one actually has to deal with a three state tunneling mechanism. Nevertheless the tunneling period can still be calculated via (27) quite accurately.

We illustrate this by means of the resonance at $N \approx 33$ where T_{tunnel} changes about two orders of magnitude. The Husimi distributions of the three Floquet states

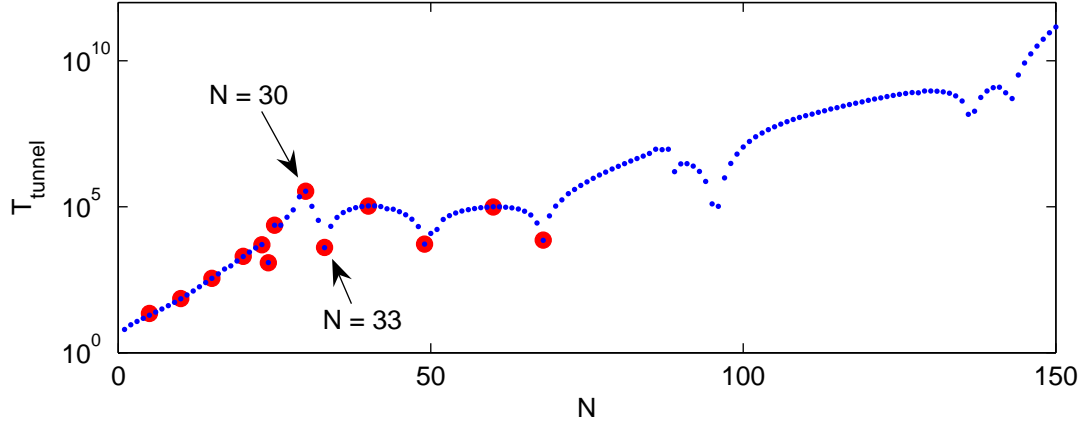


Figure 6. Tunneling period T_{tunnel} calculated from $\Delta\epsilon$ according to (27) as a function of N for $\varepsilon = 0$, $v = 1$, $\tau = 1$ and $c = 2/(N + 1)$ fixed; \bullet T_{tunnel} determined from numerical propagation

$|\kappa_{\pm}\rangle$ and $|\kappa_c\rangle$ involved in the tunneling for $N = 33$ are shown in figure 7. The third state $|\kappa_c\rangle$ is mostly localized in the chaotic regions of the classical phase space and may therefore be denoted as “chaotic” state. The overlap of this state with the island states is actually small, $|\langle\kappa_c|\pm\rangle|^2 \approx 0.06$. Nevertheless it changes the behaviour of the system dramatically. To visualize the tunneling process, it is sufficient to focus on the z -component during propagation. In figure 8 the z -component is shown for $N = 30$ and $N = 33$. The great difference in the tunneling period is obvious here. The system with $N = 30$ particles shows perfect self-trapping up to 10^4 kick periods, whereas the system with just three more particles exhibits strong tunneling with $T_{\text{tunnel}} \approx 4000\tau$. Thus, the small variation of the number of particles obviously changes the entire tunneling process from a two state to the three state mechanism. If one takes a closer look on the tunneling oscillations of this system the small modulations attract attention. These can easily be understood as tunneling into the third state $|\kappa_c\rangle$ which is superimposed. The period T_c of these modulations can be calculated by the means of (27) with the quasi energy splitting $\Delta\epsilon_c$ between the third level and the tunneling doublet. In this concrete case this yields $T_c = 551$ in perfect agreement with the numerical propagation.

To get a sophisticated impression of the behaviour of the quasi energies, especially crossing or avoided crossing scenarios in regions where the levels really get close to each other, one needs to examine their dependence on continuous variables e.g. the kick strength c . Of special interest is the role of the third chaotic state. One has to keep in mind, however, that the mean-field phase space structure changes by varying c ; especially both of the regular islands are modified. At first we take a look at the tunneling time T_{tunnel} as a function of c where we leave the number of particles $N = 30$ fixed. This case is shown in figure 9. This plot provides similar features as seen for the N -dependence in figure 6. For small values of c the tunneling period increases faster than exponential and shows an almost monotonous behaviour. For $c \lesssim 2/(N + 1)$ a

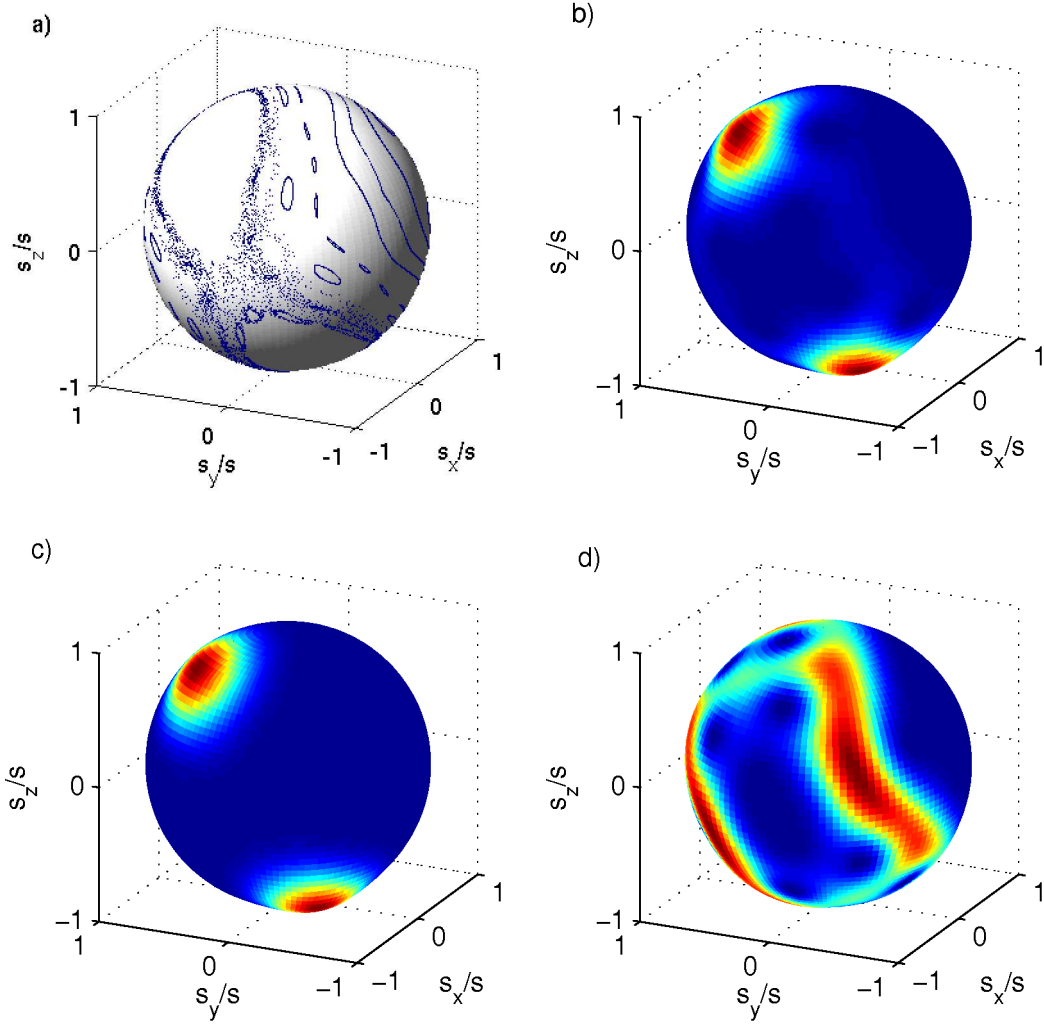


Figure 7. The three tunneling states for $N = 33$, $\varepsilon = 0$, $v = 1$, $\tau = 1$ and $c = 2/(N + 1)$: a) mean-field phase space , b) Husimi distribution $|\langle \vartheta, \varphi | \kappa_+ \rangle|^2$, c) $|\langle \vartheta, \varphi | \kappa_- \rangle|^2$, d) $|\langle \vartheta, \varphi | \kappa_c \rangle|^2$

sharp peak can be observed which in fact is a divergence. This phenomenon is known under the key word “coherent destruction of tunneling” (CDT) [31]. At these points in parameter space the two levels belonging to the tunneling doublet cross. Since they have different parity such crossings are not forbidden. This zero splitting automatically leads to a divergence in the tunneling period.

For higher values of c there also exist the same kind of resonances as seen in dependence of N , where the tunneling period decreases about several orders of magnitude. They are due to avoided crossing scenarios of the quasi energy levels. In figure 10 we show the quasi energies over the interaction strength c for $N = 30$ particles (note the cylindrical topology of the plot; due to the definition of the quasi energies $-\pi$ and π have to be identified on the ϵ -axis). Let us focus on the prominent resonance at $c(N + 1) \approx 2.35$ corresponding to the region marked with (2). A blow-up of this

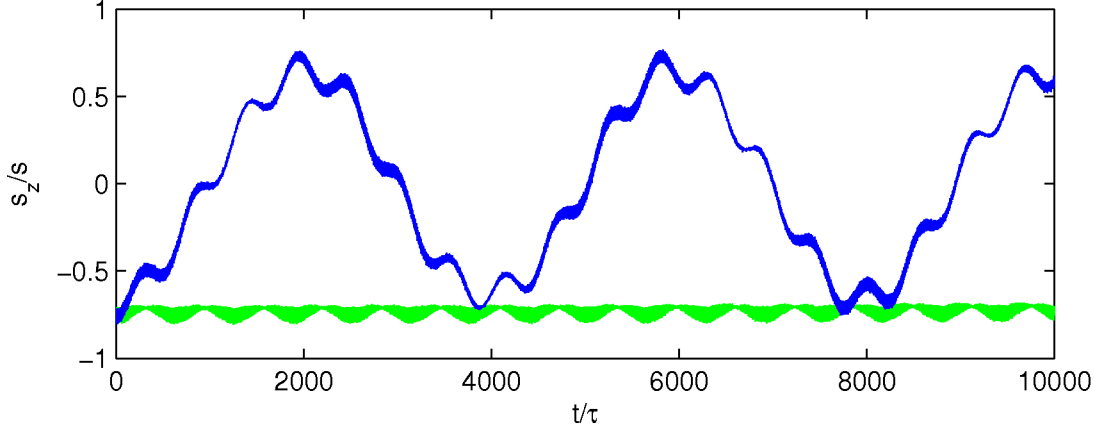


Figure 8. Behaviour of the population imbalance $\langle L_z \rangle / l$ over 10000 kick periods for $\varepsilon = 0$, $v = 1$, $\tau = 1$ and $c = 2/(N + 1)$; — $N = 30$ particles, — $N = 33$ particles

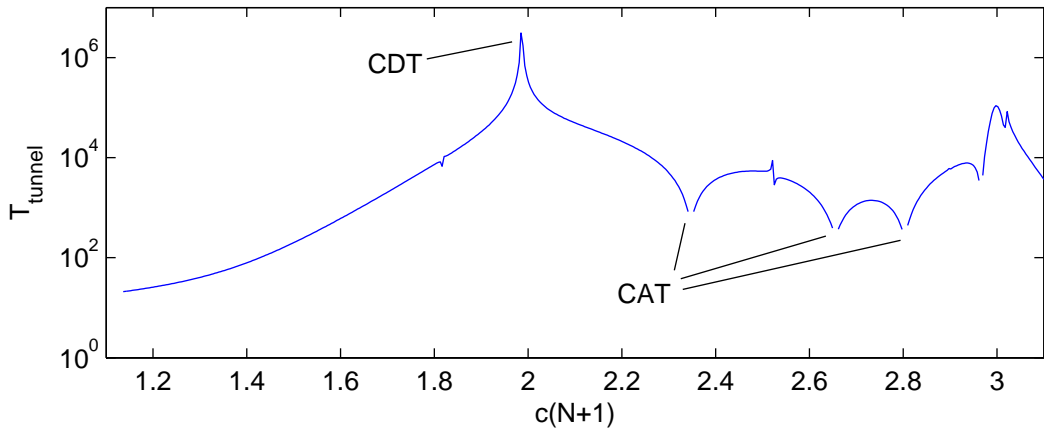


Figure 9. Tunneling time T_{tunnel} calculated according to (27) with the help of $\Delta\epsilon$ as a function of c for a fixed number of $N = 30$ particles, $\varepsilon = 0$, $v = 1$ and $\tau = 1$; CDT: coherent destruction of tunneling divergencies, CAT: chaos assisted tunneling resonances, in the regions of the small gaps the two state approximation breaks down.

region is shown on the right-hand side of figure 11. Here one of the levels of the doublet undergoes an avoided crossing with a chaotic third level ϵ_c since they belong to the same symmetry class. The splitting of the avoided crossing is in the same order of magnitude as the splitting of the tunneling doublet. Hence, in an intermediate region the three states $|\kappa_{\pm}\rangle$ and $|\kappa_c\rangle$ all take part in a three state tunneling mechanism. The simple two state model breaks down here and the tunneling time cannot be evaluated according to (27) (note the small gaps in the graph in figure 9). Due to the strongly avoided crossing the splitting of the tunneling doublet increases, when the third state approaches, which causes a significant decrease of the tunneling time on the other hand. This stimulated tunneling process is often called chaos assisted tunneling (CAT) because of the participation of the chaotic state $|\kappa_c\rangle$ [32, 33].

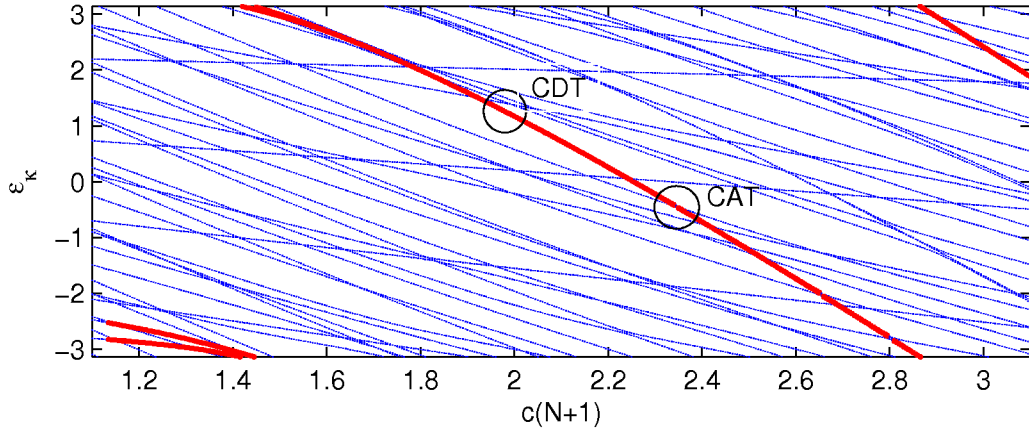


Figure 10. Quasi energies ϵ_κ for $N = 30$ particles, $\varepsilon = 0$, $v = 1$ and $\tau = 1$ as a function of c ; • tunneling doublet ϵ_\pm ; (CDT): real crossing of ϵ_\pm inducing CDT; (CAT): avoided crossing with a chaotic level inducing CAT, see text for details.

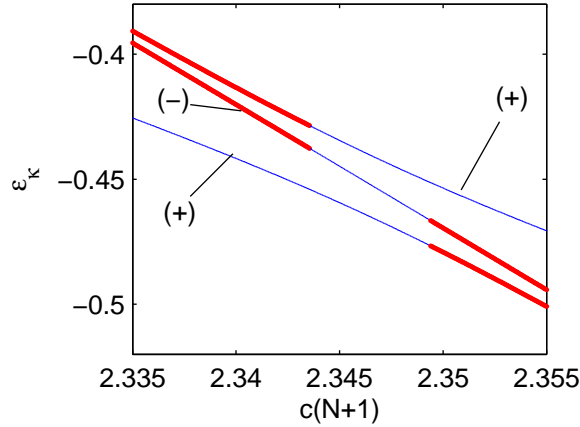


Figure 11. Blow-up of the CAT region of figure 10; the symmetry of the quasi-energy levels are denoted by (\pm) ; one observes an avoided crossing of the quasi-energy levels with $(+)$ -symmetry; • tunneling doublet ϵ_\pm .

Comparing the Figures 10 and 9 it becomes obvious that apart from these resonant avoided crossing events there is a large number of avoided crossings which have no significant influence on the tunneling period. The avoided crossing between the third level and one of the doublet levels has only a very small splitting in these cases, which has no influence on the tunneling period, since the quasi energy doublet stays almost undistorted.

6. Tunneling landscapes

Canonical transformations for the Floquet operator (4) are mappings under which the eigenvalues and symmetry properties of F are preserved. For the present system these are given by orthogonal matrices. Therefore F has the codimension $n = 2$, which means

that at least two system parameters have to be varied to enforce a degeneracy of two quasi energies belonging to the same symmetry class [34, 35]. As one parameter one may choose the interaction strength c ; the second parameter is the time scale of the system which is given by the single particle tunneling frequency v . Hence accidental degeneracies of such quasi energy planes $\epsilon_\kappa(c, v)$ occur at most at isolated points in the parameter space spanned by c and v . However, planes belonging to *different* symmetry classes, i.e. having opposite parity, actually exhibit exact crossings which form a one dimensional manifold in the (c, v) -plane. Thus, the quasi energy planes $\epsilon_\kappa(c, v)$ cross along lines [31]. These lines play an important role in the context of the tunneling since the tunneling period T_{tunnel} diverges there. Plotting T_{tunnel} as a function of c and v yields the “tunneling landscape” of the kicked double-well BEC. Figure 12 shows $T_{\text{tunnel}}(c, v)$ in false colour representation on a logarithmic scale. One observes indeed a rich landscape with diversified sequences of ridges and valleys. The sharp lines with small values of the tunneling period (dark blue) correspond to the CAT regions; along these lines avoided crossings of the quasi energy planes with significant splitting occur. On the other hand, the sharp lines with high values of T_{tunnel} are actually lines of divergence since the quasi energy planes intersect along these lines in parameter space. Thus they correspond to the CDT regions. In the upper left corner of the presented section of parameter space, i.e. for smaller values of c and larger values of v , regular dynamics prevails and almost no crossings of the quasi energy planes take place. The consequence of which is a flat tunneling landscape area. The opposite holds in the chaotic regime; here a larger number of CAT resonances and CDT divergences occur. Remarkable is the new kind of “avoided crossings” between both the ridges and the valleys of the landscape. Some of these are shown in figure 13 which are blow-ups of figure 12. A systematical feature at these crossings is the direct neighbourhood of resonances and divergences which could already be observed in figure 9 which is actually a cut through figure 12 at $v = 1$. Another interesting fact about this tunneling landscape is, that in principle the system can also be tuned to the CDT regime by adjusting one parameter. Thus for this kicked system real self-trapping is possible not only in the mean-field regime, but also for the full quantum system.

7. Conclusion

In the present paper we investigated a two mode BEC with a periodically kicked interaction term in a many-particle as well as in a mean-field description. This system is actually equivalent to the kicked top which is a standard example of quantum chaos. Besides the new answer to the question if the kicked top can be realized experimentally, this new context shed light on different aspects of the model. We showed that the tunneling oscillations of the many-particle system which usually suppress the self-trapping effect show a rich spectrum of phenomena like coherent destruction of tunneling and chaos assisted tunneling. The sensitive parameter dependence of the tunneling behaviour of the system offers an interesting tool for the manipulation of Bose-Einstein

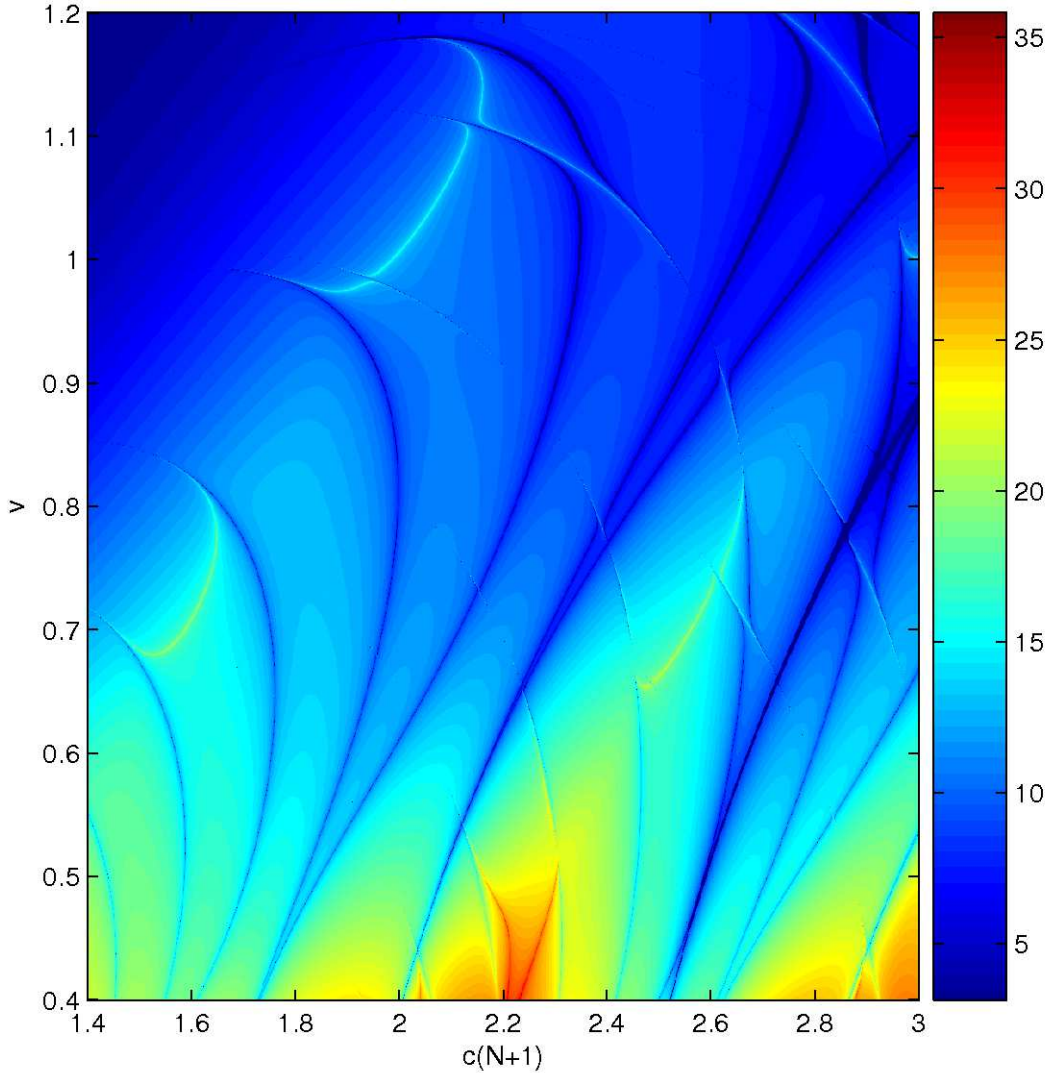


Figure 12. Tunneling landscape, T_{tunnel} over (c, v) in false colour representation on logarithmic scale; $N = 30$ particles, $\varepsilon = 0$ and $\tau = 1$; the sharp lines with small tunneling times represent CAT regions whereas these with high values of the tunneling time represent CDT regions.

condensates.

- [1] M. H. Anderson, J. R. Ensher, M. R. Matthews, C. E. Wieman, and W. E. Cornell, *Science* **269** (1995) 198
- [2] K. B. Davis, M. O. Mewes, M. R. Andrews, N. J. van Druten, D. S. Durfee, D. M. Kurn, and W. Ketterle, *Phys. Rev. Lett.* **75** (1995) 3969
- [3] M. Albietz, R. Gati, J. Fölling, S. Hunsmann, M. Cristiani, and M. K. Oberthaler, *Phys. Rev. Lett.* **95** (2005) 010402
- [4] I. Bloch, *Nature Physics* **1** (2005) 23
- [5] J. R. Anglin and A. Vardi, *Phys. Rev. A* **64** (2001) 013605

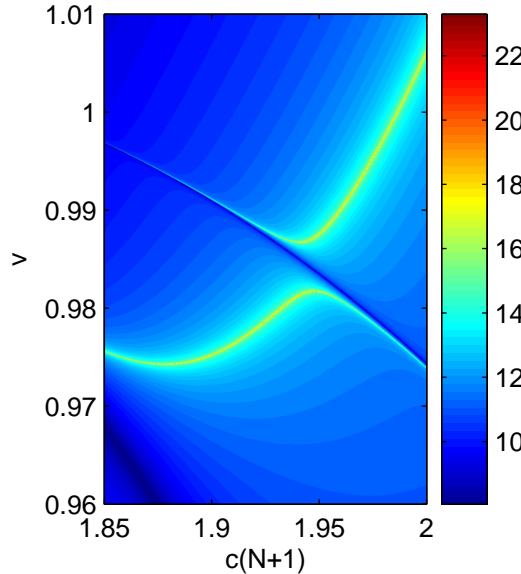


Figure 13. Tunneling landscape, blow-up of figure 12; avoided crossing of two CDT ridges, in the gap one observes a CAT valley.

- [6] K. W. Mahmud, H. Perry, and W. P. Reinhardt, Phys. Rev. A **71** (2005) 023615
- [7] S. Mossmann and C. Jung, Phys. Rev. A **74** (2006) 033601
- [8] Biao Wu and Jie Liu, Phys. Rev. Lett. **96** (2006) 020405
- [9] H. J. Korsch and E. M. Graefe, Phys. Rev. Lett. (2006) submitted (preprint: quant-ph/0611040)
- [10] F. Haake, M. Kuś, and R. Scharf, Z. Phys. B **65** (1986) 381
- [11] F. Haake, *Quantum Signatures of Chaos*, Springer, Berlin, Heidelberg, New York, 2001
- [12] F. Haake, Journal of Modern Optics **47** (2000) 2883
- [13] G. J. Milburn, J. Corney, E. M. Wright, and D. F. Walls, Phys. Rev. A **55** (1997) 4318
- [14] M. Holthaus and S. Stenholm, Eur. Phys. J. B **20** (2001) 451
- [15] Q. Xie and W. Hai, Eur. Phys. J. D **33** (2005) 265
- [16] F. T. Arecchi, Eric Courtens, Robert Gilmore, and Harry Thomas, Phys. Rev. A **6** (1972) 2211
- [17] A. M. Perelomov, *Generalized Coherent States and Their Applications*, Springer, Berlin Heidelberg New York London Paris Tokyo, 1986
- [18] M. Holthaus, Phys. Rev. A **64** (2001) 011601
- [19] W. A. Lin and L. E. Ballentine, Phys. Rev. Lett. **65** (1990) 2927
- [20] W. A. Lin and L. E. Ballentine, Phys. Rev. A **45** (1992) 3637
- [21] R. Bavli and H. Metui, Phys. Rev. A **47(4)** (1993) 3299
- [22] L. Bonci, A. Farusi, P. Grigolini and R. Roncaglia, Phys. Rev. E **58(5)** (1998) 5689
- [23] V. Averbukh, Shmuel Osowski, and N. Moiseyev, Phys. Rev. Lett. **89** (2002) 253201
- [24] W. K. Hensinger, A. G. Truscott, B. Upcroft, N. R. Heckenberg, and H. Rubinsztein-Dunlop, J. Opt. B **2** (2000) 659
- [25] W. K. Hensinger et. al., Nature **412** (2001) 52
- [26] W. K. Hensinger et. al., Phys. Rev. A **64** (2001) 033407
- [27] D.A. Steck, W. H. Oskay, and M. G. Raizen, Science **293** (2001) 274
- [28] S. Osowski and N. Moiseyev, Phys. Rev. A **72** (2005) 033603
- [29] A. P. Hines, R. H. McKenzie, and G. J. Milburn, Phys. Rev. A **71** (2005) 042303
- [30] J. Y. Shin and H. W. Lee, Phys. Rev. E **50** (1994) 902
- [31] M. Grifoni and P. Hänggi, Phys. Rep. **304** (1998) 229
- [32] S. Tomsovic and D. Ullmo, Phys. Rev. E **50(1)** (1994) 145

- [33] S. Kohler, R. Utermann, P. Hänggi and T. Dittrich, Phys. Rev. E **58**(6) (1998) 7219
- [34] E. P. Wigner, *Group Theory and its Applications to the Quantum Mechanics of Atomic Spectra*, Academic, New York, 1959
- [35] F. J. Dyson, J. Math. Phys. **3** (1962) 140, 157, 166